The optical design of a 10-meter cryogenic interferometer

Student number: 2325410D

2325410d@student.gla.ac.uk

University *of* Glasgow

Abstract. With the detection of gravitational waves, laser interferometry has become an increasingly active area of interest for physicists. Since the first iteration of detection hardware is nearing the limit, newer detection methods and hardware is required. Prototype models of interferometers with altering designs are being developed to combat this detection limit. This paper investigates an optimal optical layout for one such prototype currently in development by the Institute of Gravitational Research at the University of Glasgow. A python simulation of the setup was constructed for both cavities, producing an optimal cost-effective configuration. For the reference cavity, lenses of focal length -1.750m and 2.5m are required. Likewise, four lenses of focal lengths -0.430m, 1.875m, 2.500m and 0.350m, respectively- are necessary for the cryogenic cavity. The final expenditure for each cavity is unknown since both cavities require custom-made lenses within manufacturing capabilities. An approximate expenditure of £100 for the reference cavity and £160 for the cryogenic cavity was assumed. Evaluation of the solution proposed was achieved by performing mode-matching. A final variance of 0.1μm and 7.43μm was observed for the cryogenic waist and reference waist, respectively.

Acknowledgements

I would like to thank both Dr Stephen Webster and Dr Eric Oelker for their continued supervision and support during this project. Stephen and Eric always took the time to review and critique the many lines of code submitted week by week. Anytime I was perplexed by an issue, I felt comfortable expressing my thoughts and concerns to them.

To my academic supervisor, Dr Pedro Miguel Parreira, thank you for your continued support throughout the final year of my degree. I am forever grateful for the guidance given to me this past wild year.

To my friends, thank you all for the trips to the pub, the many, many games of pool played, and the fun-filled game nights. I am so glad I got the opportunity to make those memories with you. Thank you for persisting with my antics and keeping me on the straight and narrow.

To my family, I cannot thank you all enough for your never-ending love and support. Dad, Mum, Maddy and Andrew have always been there supporting and encouraging me throughout my life. I would be a completely different person without anyone of them being present in my life right now.

1. Introduction

Since their first detection in late 2015 [1], physicists have been increasingly intrigued by the elusive nature of gravitational waves. Summarised, gravitational waves can be thought of as disturbances in the curved nature of spacetime. These waves can only be generated from supermassive objects accelerated to extreme speeds. It was the detection in 2015 that solidified the theory of gravitational waves, initially proposed far earlier [2]. This detection was first established by LIGO, the laser interferometer gravitational-wave observatory. The event that triggered the release of the detectable gravitational wave was a black hole merger event. Since the detection in 2015, laser interferometry has been at the forefront in detecting such disturbances. As gravitational astronomy has evolved, significant improvements have been made in detecting such disturbances [3]. Further funding has allowed the development of small-scale prototype interferometers to improve the next generation of hardware. Such a prototype is currently being developed within the University of Glasgow by the Institute of Gravitational Research.

Currently, the prototype is a 10m cryogenic interferometer that lacks any optical layout. It consists of two reference cavities, a 10m long reference cavity and a shorter 9.8cm cryostat cavity. The setup consists of 5 main mounting tanks for lenses, the final one encased within cryogenic refrigeration. A laser is then passed via optical cable into the first tank and split into two distinct beams.

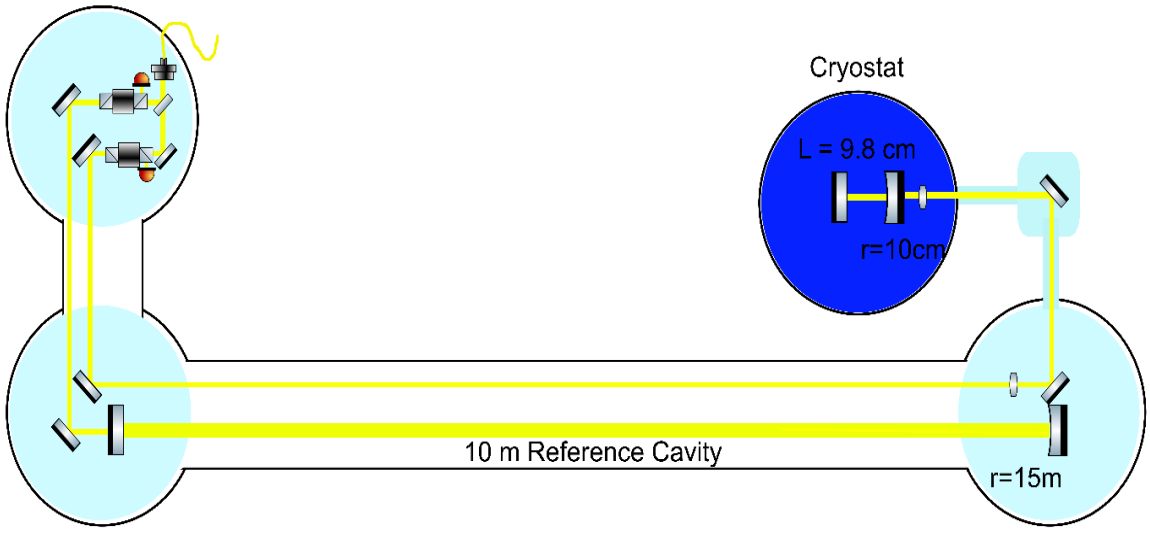

Figure 1: Pictorial rendering of apparatus. Details of cavity lens for both the reference and cryogenic cavities are given.[4]

As illustrated, one beam passes directly into the 10m reference cavity. The other beam propagates through the system and passes directly into the cryogenic cavity. It was advised that the initial beam size upon entering the system was 1mm, and the wavelength utilized will be 1550nm. At 1550nm, silicon is effectively transparent [5]. The radii of curvature for the beam at each cavity was also supplied, 15m and 10cm for the reference and cryogenic cavities. The aim is to achieve an optimal optical layout for the setup described, a setup that is both reliable and cost-effective. Python simulations of the setup may be made to achieve the desired configuration.

2. Background Theory

To first form a basis in tackling the design problem, a fundamental understanding of three key aspects must exist. These three aspects are; Gaussian beams, Gaussian beam propagation and the process of

mode matching. In essence, an understanding of how a beam is described, propagated and then evaluated throughout an optical system must exist.

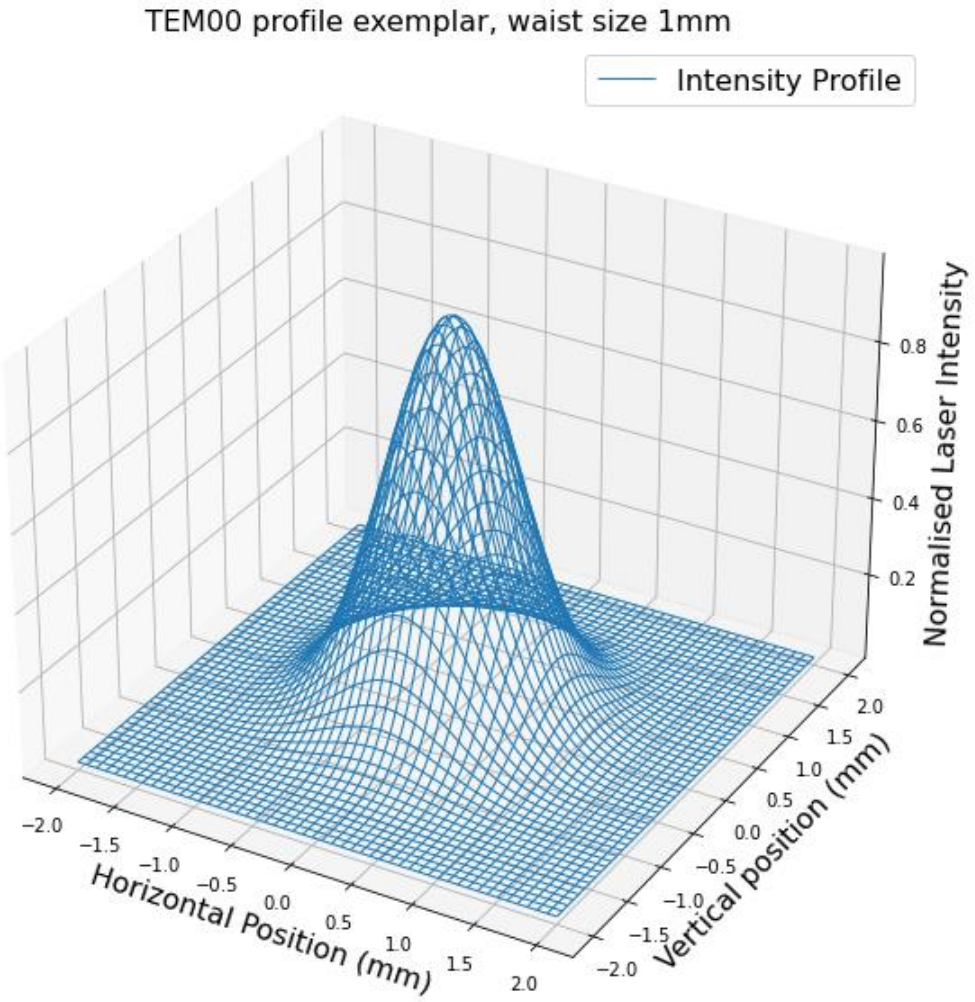

Figure 2: Normalized intensity profile for a laser striking a flat surface. The shape produced is the fundamental Gaussian mode for a waist size 1mm beam. Figure reconstructed from [6].

2.1. Gaussian Beams

Generally, the intensity output of a laser may be modelled by a Gaussian distribution hence the term Gaussian beam. Consider a laser propagating through empty space; if cross-sections of the beam are taken at regular intervals along the propagation axis, each intensity distribution forms a gaussian curve [7]. Mathematically, the fundamental Gaussian mode, TEM00, which describes the production of a laser exactly, may be modelled as such:

$$\mathbf{E}(r,z) = E_0\hat{\mathbf{x}}\frac{w_0}{w(z)}\exp\left(\frac{-r^2}{w(z)^2}\right)\exp(-ikz)\exp\left(\frac{-ikr^2}{2R(z)}\right)\exp(-iG(z)) \quad (1)$$

With an origin defined at the beam waist, the narrowest part of the Gaussian beam, the beam size at any given point along the propagation axis is given by w(z). For the waist size, propagation

distance may be set to zero provided a function w(z) has been solved. As the beam propagates forward, the front of the beam begins to curve as the beam size increases; the term describing such curvature is given as R(z). The function also picks up an additional phase term, the Gouy Phase, G(z). This term arises because gaussian wave propagation can be described as a superposition of waves propagating in the alternate axis of propagation [8].

2.1.1. *Common formalisms.* The confocal parameter, otherwise known as the Rayleigh range, is imperative for describing three critical factors of Gaussian beams. The Gouy phase, beam size and radius of curvature may all be described in terms of the confocal parameter b.

$$b = \frac{\pi w_0^2}{\lambda} \tag{2}$$

For a fixed laser beam of wavelength λ and waist size w_0 the confocal parameter remains unchanged. Moreover, it is possible to construct equations to describe the beam size, curvature radius, and Gouy phase from the confocal parameter.

$$w(z) = w_0 \sqrt{1 + \left(\frac{z}{b}\right)^2} \tag{3}$$

$$G(z) = \tan^{-1}\left(\frac{z}{b}\right) \tag{4}$$

$$R(z) = \frac{b^2 + z^2}{z} \tag{5}$$

The complex beam parameter is another standard formalism that is extremely versatile in describing Gaussian beams. Describing the beam in terms of both real and imaginary components allows for seamless analysis of Gaussian beam interactions between optical elements.

$$q(z) = z - ib \tag{6}$$

The real component of this complex beam parameter, commonly dubbed the q-value, denotes the distance along the z-axis from the waist origin. As previously defined, the imaginary part is the confocal parameter. Expressing the beam in this form allows for massive simplification when propagation mathematics is concerned. Beam propagation is simplified to behave like an ordinary ray in this form. Using the set of equations (2-6), a Gaussian beam may be fully described throughout an optical system. This set also allows for a considerable amount of simplification to be achieved during the beam propagation. This set of tools does not describe how the beam interacts with certain optical elements; hence a method for beam propagation is required.

2.2. Beam Propagation

To propagate any ray throughout a system, two pieces of information must be known, the overall ray transfer matrix and the configuration of the ray before entering the system [9]. Propagating a Gaussian beam is no different. The beam state before entering a system may be given as the q-value of the beam. Each optical element within a system has an associated ray transfer matrix. These matrices govern how an incoming beam will behave after successful interaction with the corresponding optical element. If the system has multiple optical components, for instance, free space followed by a lens followed by free space, the transfer matrix is the product of these matrices. However, it is essential to note that the order matters in multiplying ray transfer matrices. In general, for a system of *i* elements, the overall ray transfer matrix is the product of the matrices Mn to M1 in reverse order of propagation. The output state of a beam can therefore be described as the ray transfer matrix acting on the initial beam state and expressed as:

$$M_{transfer} = M_i M_{i-1} \dots M_1 \tag{7}$$

$$\begin{pmatrix} q_{output} \\ 1 \end{pmatrix} = M_{transfer} \begin{pmatrix} q_{input} \\ 1 \end{pmatrix} \tag{8}$$

If the initial state of the beam is known for an optical system, then by applying the associated ray transfer matrix, a solution for the output beam state may be found. After solving the output beam state, equations 2-6 can be applied to give a more detailed analysis of the beam interaction. This allows for analysis of beam size and radii of curvature just before and immediately after optical elements. Using the formalisms for Gaussian beams and beam propagation, it is now possible to fully simulate an optical system. To assess the reliability of the simulation, a further tool must be implemented; mode-matching.

2.3. Mode-matching

Qualitatively mode-matching is a consistency check between two beams. If two beam profiles are consistent, then a high value of mode-matching is attained. Essentially it is how well the spatial distributions of the two beams overlap. As expressed in the name, mode-matching matches the q-value from one optical element to another. Mathematically it is described as the overlap integral between two spatial distributions and is defined as such [9]:

$$\eta = \frac{\left|\int_A E_1^* E_2 dA\right|}{\int_A |E_1|^2 dA \int_A |E_2|^2 dA} \tag{9}$$

In this case, η ranges from zero to one, the higher the value of η attained indicate a higher-quality mode match, spatial distributions are similar. Equation 9 may instead be written in terms of the q-value for each beam:

$$\eta = \frac{\sqrt{(q_{x1} - q_{x1}^*)(q_{y1} - q_{y1}^*)(q_{x2} - q_{x2}^*)(q_{y2} - q_{y2}^*)}}{|q_{x2} - q_{x1}^*|\left|q_{y2} - q_{y1}^*\right|} \tag{10}$$

It can be shown that equation 9 may be transformed into equation 10 [10]. This expression also accounts for the possibility of astigmatism occurring within the setup. By expressing the mode-

matching value in terms of q-values, an optical design may be simulated, but the tolerances on solutions may also be known. Mode-matching may also be carried out between each lens. This would indicate which lenses need to be optimized and the degree of accuracy they need to be solved. The quicker an approximate solution deviates from the exact answer, the tighter the tolerance is for that specific lens. With knowledge of Gaussian beams, beam propagation and mode-matching, it is now possible to form simulations of the proposed setup and assess the solutions achieved via the simulations.

3. Design Process

The main goal was to establish an optimal optical layout for the reference cavity and cryogenic cavity. Once a configuration is found, the required lens specification must then be available via laserOptik, a site specialising in fabricating lenses [11]. To begin solving for optimal layouts, the waist size at the end of each cavity must be known along with their confocal parameters. Using equations 2 and 5, both confocal and waist size properties may be derived.

Table 1. Reference cavity and cryogenic cavity details as calculated from the initial values provided in Figure 1.

Resonator Cavity	Confocal Parameter	Waist Size
Reference Cavity (10m)	7.071m	1.868mm
Cryogenic Cavity (9.8cm)	14mm	83.11μm

The initial beam size entering the system was assumed to be 1mm with a wavelength of 1550nm. A complete python simulation of both the reference cavity and cryogenic cavity may be formed with this basic information.

3.1. Methodology

Due to the restrictions imposed by the recent Covid-19 pandemic, much of the research conducted had to be performed remotely. To alleviate the restrictive nature of the project, a python simulation of the setup was constructed using the information derived and uploaded to a private GitHub for collaborative purposes.

A general beam class was initialized with methods to call on beam properties such as beam size and defocus at specific points along the propagation axis. Ray transfer matrices were also defined for each optical element, one for empty space and another for a thin lens. A propagation method was also defined to allow the propagation of a q-value from one optical element to the next. Using these methods, it is possible to construct a reference and cryogenic cavity simulation.

3.1.1. *Reference Cavity.* It was assumed that a two-lens system would suffice for the reference cavity as there was limited space to mount the lenses. A two-lens system would make the setup cost less than multi-lens systems, but it is also easier to set up as there are only two points of variance.

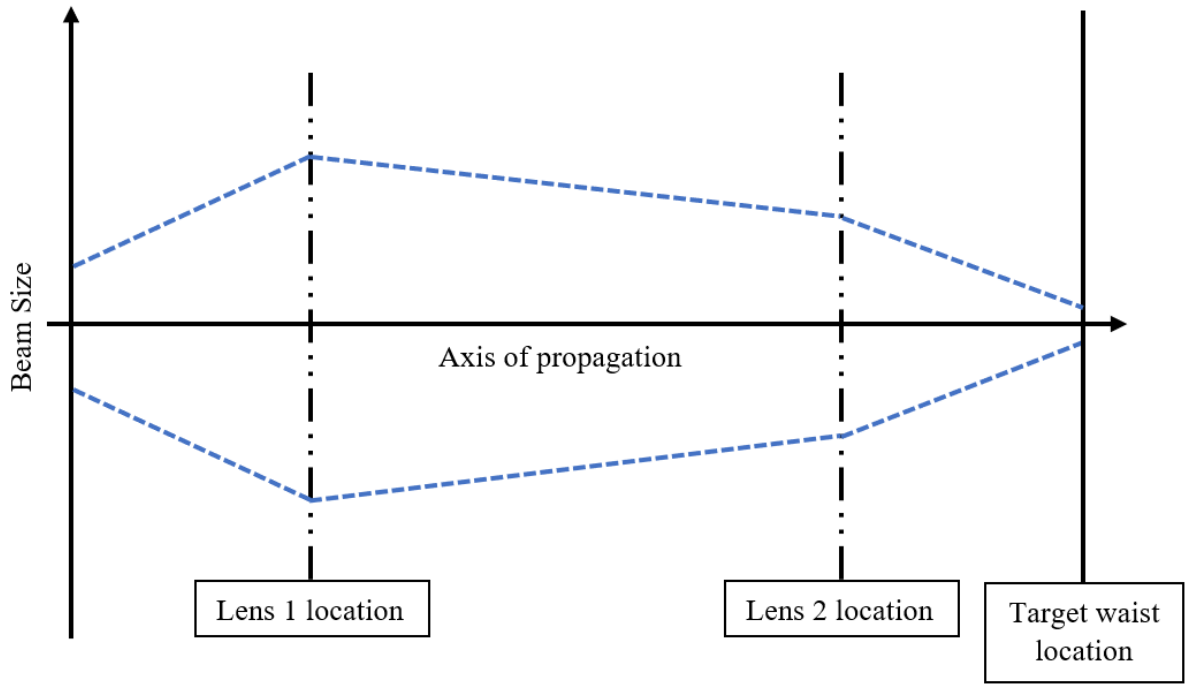

Figure 3: Pictorial sketch detailing beam size as it propagates throughout the system towards the reference cavity. The blue dashed lines indicate the varying beam size as it interacts with various optical elements.

The process for solving a two-lens system can be abstracted into three main steps. The first process is to propagate forward the initial q-value entering the system towards the first lens. The lens position is determined beforehand and is within the confines of the experimental layout. Likewise, the second step is to backpropagate the known final q-value, given from the final waist value towards the last lens in the system. Similarly, the final lens position is determined beforehand based on the physical limitations of lens locations within the layout. The final step is to generate an array of varying defocus at the first lens and propagate these to the second lens. Once propagated, the beam sizes on either side of the second lens are matched appropriately. The defocus of the beam is then noted on either side of each lens and subtracted. The resulting defocus may then be inverted to solve for the lens's focal length at that location.

Once focal lengths were achieved for both lenses, the locations of each were then iterated slightly within the confines of their platforms. This iteration was necessary to find approximate solutions which would coincide with the specification offered by laserOptik. After the approximate solution for lens properties was attained, the code was rerun with these values and mode-matched with the exact solution.

3.1.2. *Cryogenic Cavity.* Initially, it was assumed that a three-lens system would be sufficient for the cryogenic cavity; however, after a discussion on beam size control, it was far more effective to opt for a four-lens system. By having four lenses, the problem essentially becomes two two-lens optimization problems.

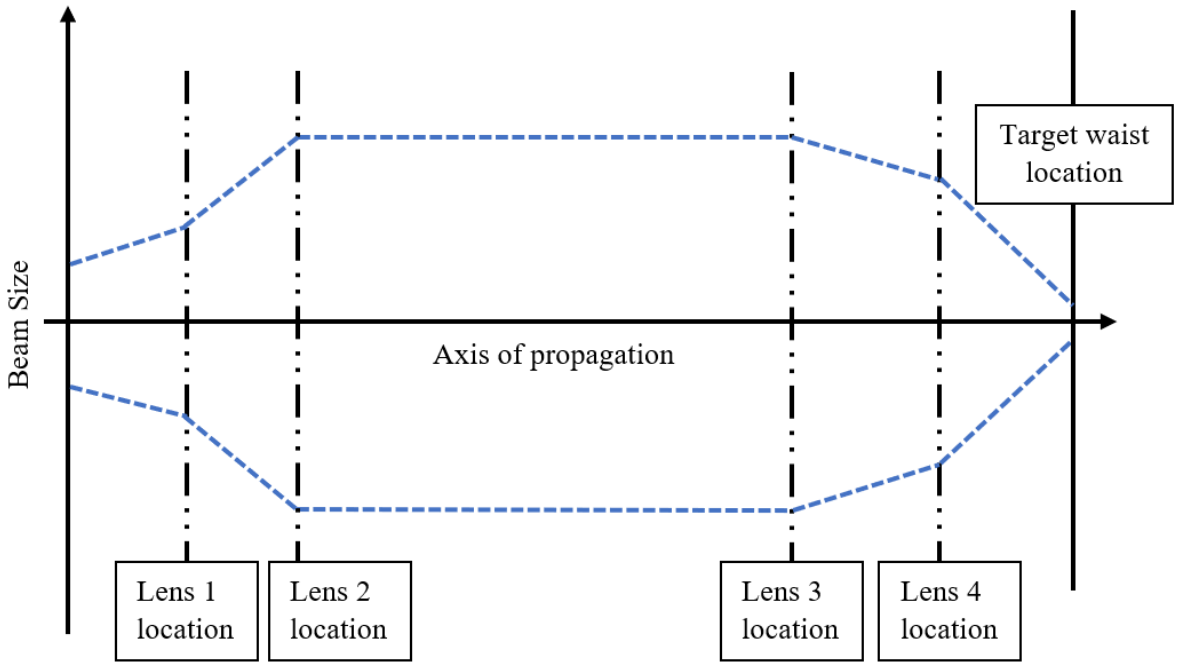

Figure 4: Pictorial sketch detailing beam size as it propagates throughout the system towards the cryogenic cavity. The blue dashed lines again indicate the varying beam size as it interacts with various optical elements. The ample space between lenses 2 and 3 show the 10m cavity.

By defining a waist between lenses 2 and 3, the optimization problem may be abstracted into two problems similar to the initial reference cavity optimization. This also allows more control over the maximal beam size throughout the system. A maximal beam size limit of 0.5cm was imposed onto the system. To comply with the limitation imposed, a waist size of 0.45cm between lenses 2 and 3 was selected.

The code structure for the reference cavity was then applied to the cryogenic cavity twice for each set of lenses. Much like the reference cavity, an exact solution was found for all four lenses. The positions of each of these lenses were then iterated slightly, again within the confines of the layout provided. After iteration, a selection of 4 approximate lenses was obtained from laserOptik. The properties of these lenses were then fed back into the script and reran to attain a mode-matching quality number for the approximate solution.

4. Results

Two sets of results were achieved for both cavities, an exact solution and an approximate solution. The approximate solution consists of lenses available from lens vendors or are within manufacturing capabilities. While it may fall within the realm of manufacturing capabilities, the exact solution would incur higher costs due to particular focal lengths.

4.1. Reference Cavity Specification

From the simulation of the reference cavity, it was determined that the first lens should be plano-concave while the final lens should be plano-convex.

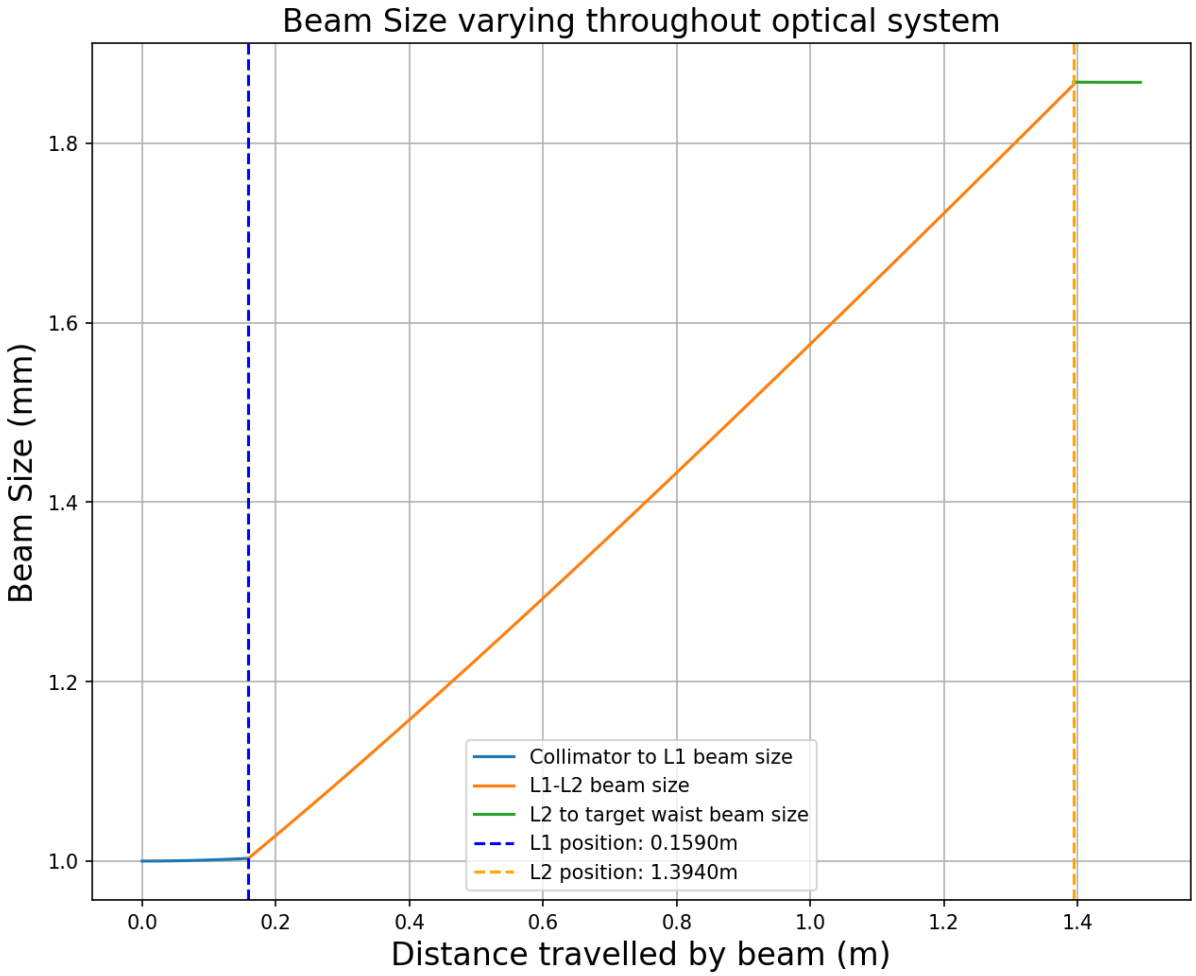

Figure 5: Beam size leading up to the reference cavity plotted against propagation distance. The solution constructed is the analytic solution. Figure produced from [12].

The beam size starts at an initial 1mm and slightly expands before interacting with lens 1. Upon interaction with lens 1 the beam diverges from tank 1 to tank 2. Within tank 2 a second lens, lens 2, converges the beam to the desired waist size of 1.868mm. After minor lens location iterations, the finalized focal lengths for lenses 1 and 2 were calculated to be -1.737m and 2.500m, respectively.

4.1.1. *Reference Cavity formal solution.* After comparing the calculated values to stock available, a focal length of 2.5m was selected for the final lens. For lens 1 an approximate value of -1.750m was obtained. This was not readily available from laserOptik but is within the realm of manufacturing capabilities. The location of lenses 1 and 2 are 0.159m and 1.394m along the axis of propagation, respectively. The total cost of this section of the experiment is expected to exceed £100.

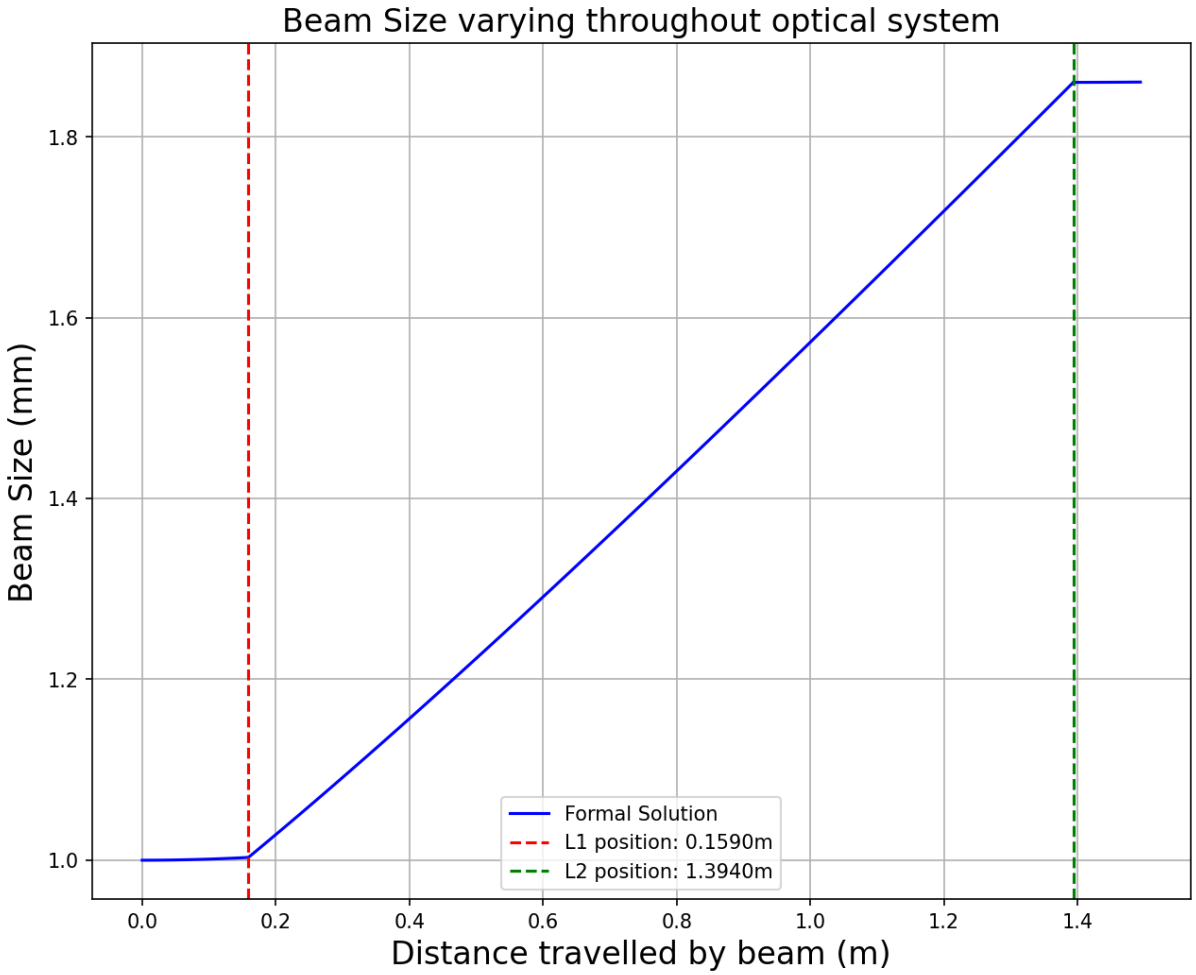

Figure 6: Beam size leading up to the reference cavity plotted against propagation distance. The solution plotted is the formal solution. Visual inspection implies that the formal solution agrees with the exact solution. Figure produced from [12].

4.2. Cryogenic Cavity Specification

A total of 4 lenses is required for the cryogenic cavity setup. The first of these lenses is plano-concave, while the latter requires a plano-convex.

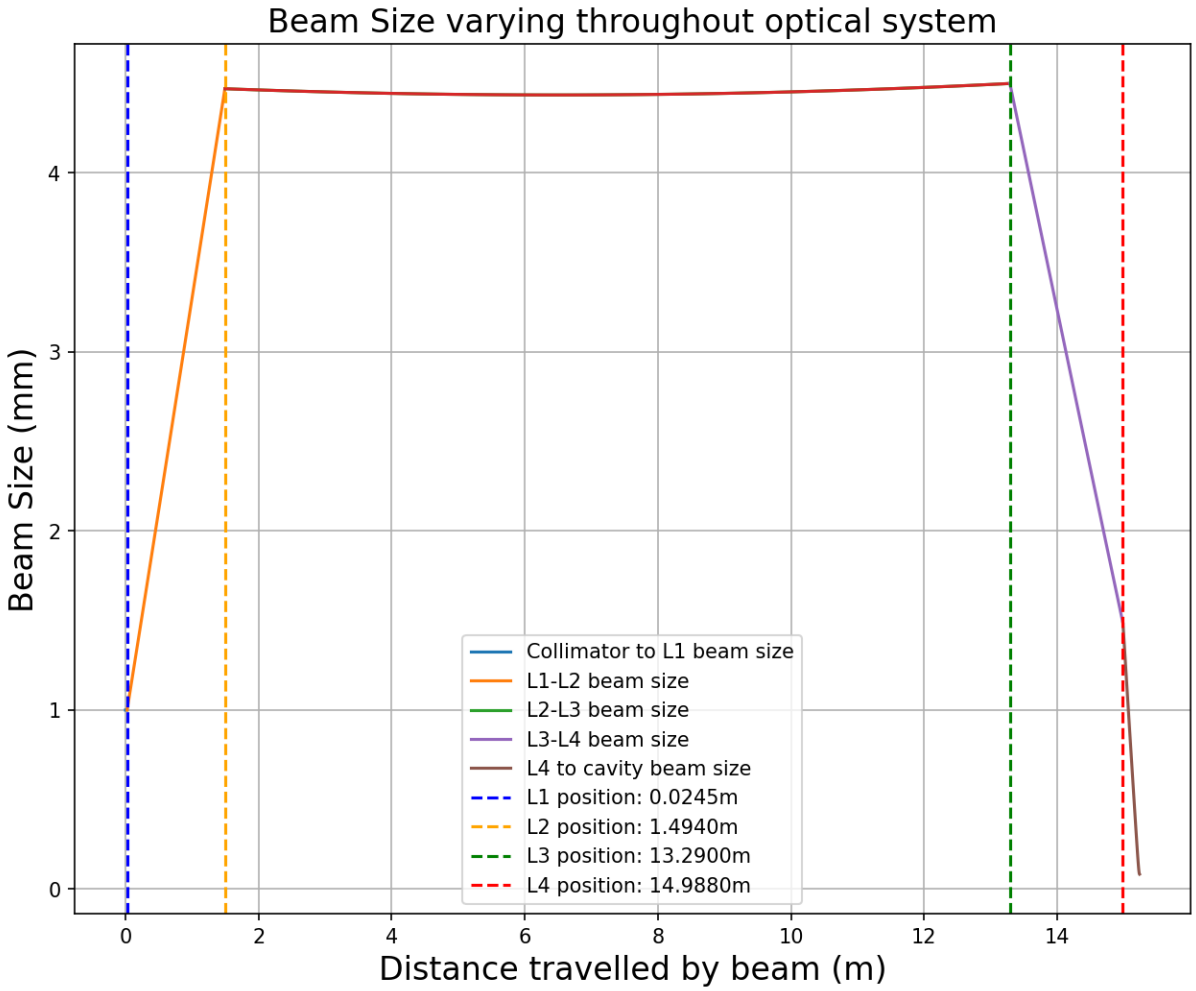

Figure 7: Beam size leading up to the cryogenic cavity plotted against propagation distance. The solution plotted is the analytic solution. Figure produced from [13].

Much like in the reference cavity, the beam initially diverges slightly until interaction with the first lens. Upon interaction, the beam size drastically increases before interaction with lens 2, which brings the beam to a waist between lenses 2 and 3. After striking lens 3 the beam size is then tapered in heavily before being acted on by lens 4. The final lens then brings the beam size to a tight waist at the required distance within the cryostat. It can be seen from figure [] that the beam comes to a waist between lenses 2 and 3 hence simplifying the optimization problem to two 2-lens optimization problems. For this solution, it is required that the final lens lies within the cryostat tank. This lens placement is necessary as it depends solely on the size of the waist required within the cryostat. Lenses 1 and 2 are within tanks 1 and 2, while lens 3 remains in the smaller fourth tank. This exact solution yielded focal lengths of -0.432m, 1.875m, 2.500m and 0.356m for lenses 1 to 4, respectively.

4.2.1. *Cryogenic Cavity formal solution.* Considering the exact solutions, lenses 2 and 3 were readily available from laserOptik. Lenses 1 and 4 required some approximation. Lens 4 may be rounded to 0.350m, and thus the majority of lenses may be sourced from laserOptik. Lens 1 will require custom tooling to be achieved. A focal length of -0.430m would be a sufficient approximation and allow the desired waist of 83μm to be achieved. Lenses 1 to 4 would be at 0.0245m, 1.4940m, 13.2900m and 14.9880m along the propagation axis, respectively. The total cost of this section of the experiment is expected to exceed £160.

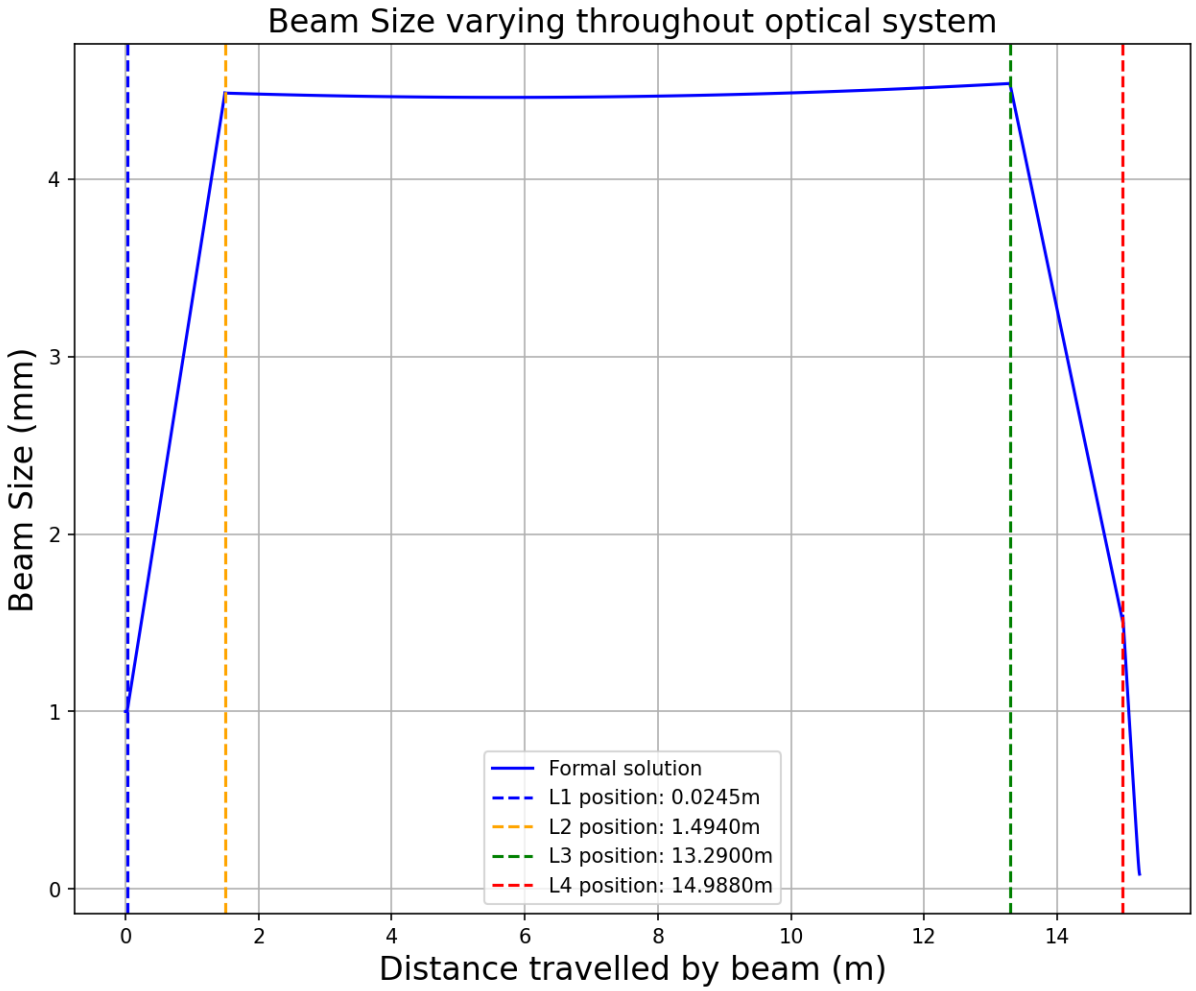

Figure 8: Beam size leading up to the cryogenic cavity plotted against propagation distance. The solution plotted is the approximate solution. Figure produced from [13].

5. Discussion

As outlined earlier, the way to qualitatively compare the approximate solution to the exact solutions derived from the simulation is via mode-matching. Once mode-matching has been calculated for each cavity, a conclusion may be drawn on the effectiveness of lens choice for each cavity.

5.1. Analytic and approximate solutions compared

After obtaining the exact focal length specifications, a rerun of the simulation was initiated. This rerun focused on varying the focal length properties within a tolerance of 15%, later adjusted to 1% for display purposes. The results were then mode-matched with the exact solutions for each cavity. The simplest of the two, the reference cavity, required only 2 lenses to be iterated over and hence took the shortest run time to compute compared to the cryogenic cavity.

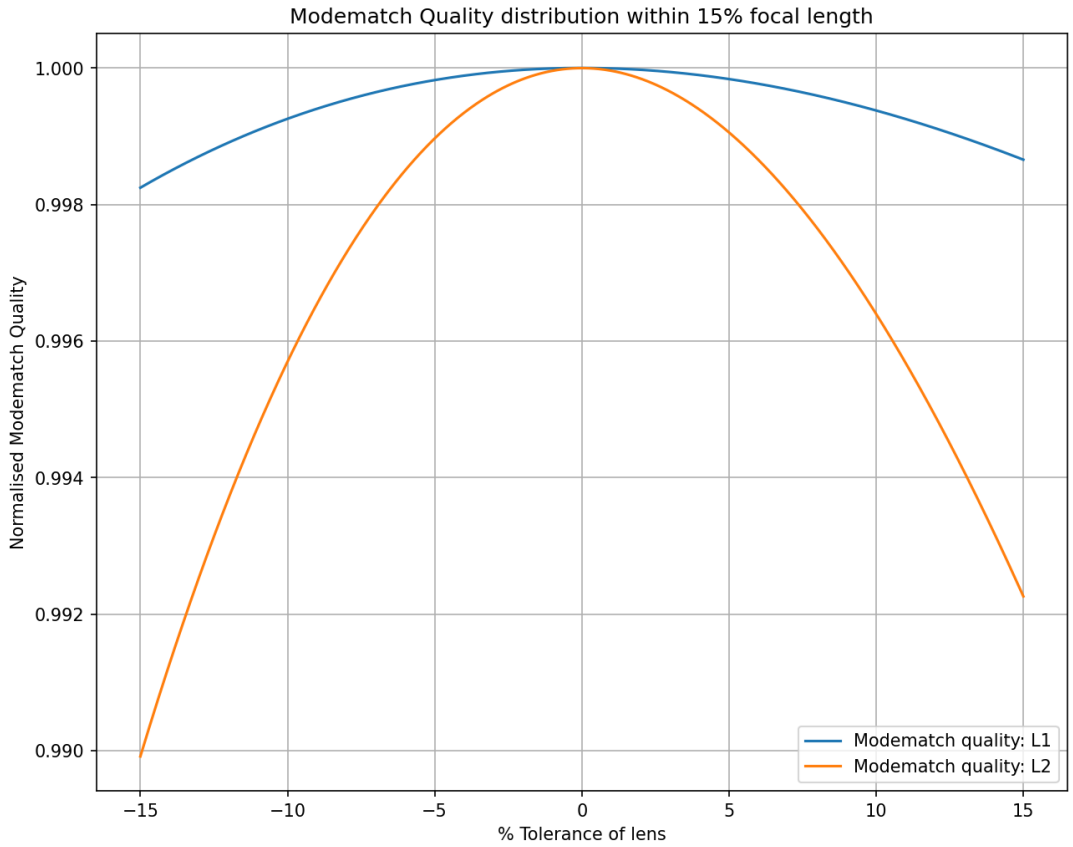

Figure 9: Mode-matching values obtained for the reference cavity. The focal lengths of each lens were iterated over a tolerance of 15%. Plot details a high mode-matching percentage within a tolerance of 5%. Figure produced from [12].

It can be seen that the mode-match quality of lens 2 begins to diverge much more quickly compared to lens 1. This indicates that the tolerances on lens 2 have to be tighter to achieve the desired waist size of 1.868mm. Lens 1 may be allowed to vary more compared to lens 2. Lens selection reflects the need for accuracy in lens 2 as it is readily available on laserOptik with a tolerance of 1%.

The more complex cavity, the cryogenic cavity, required 4 lenses to be selected appropriately. Reminiscent to the reference cavity, once exact focal lengths were known, focal lengths were iterated over a tolerance of 15% and fed back into the simulation. The resulting solutions were then mode-matched with the exact solution and analyzed. This indicates which lenses need to be manufactured to high degrees of accuracy.

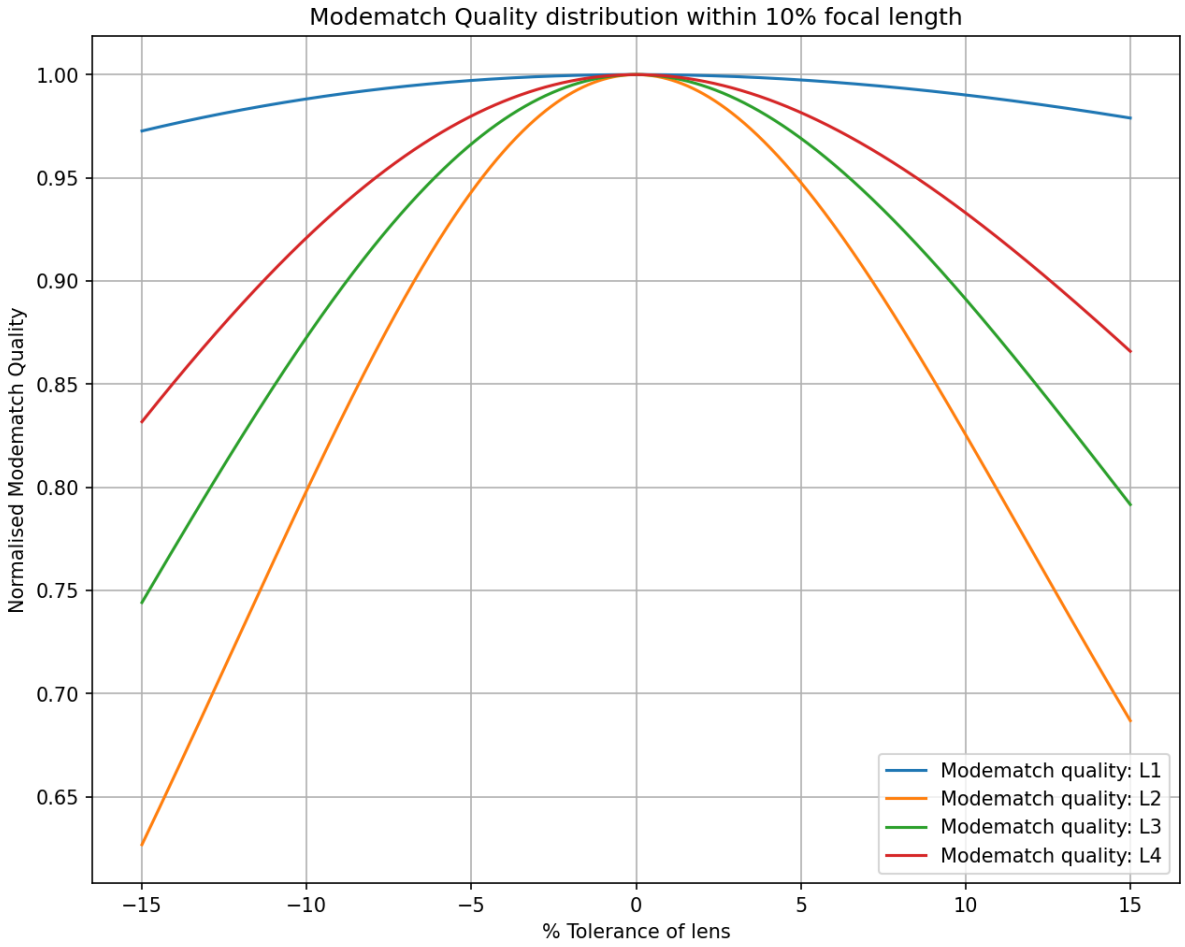

Figure 10a: Mode-matching values obtained for the cryogenic cavity. The focal lengths of each lens were iterated over a tolerance of 15%. Figure produced from [13].

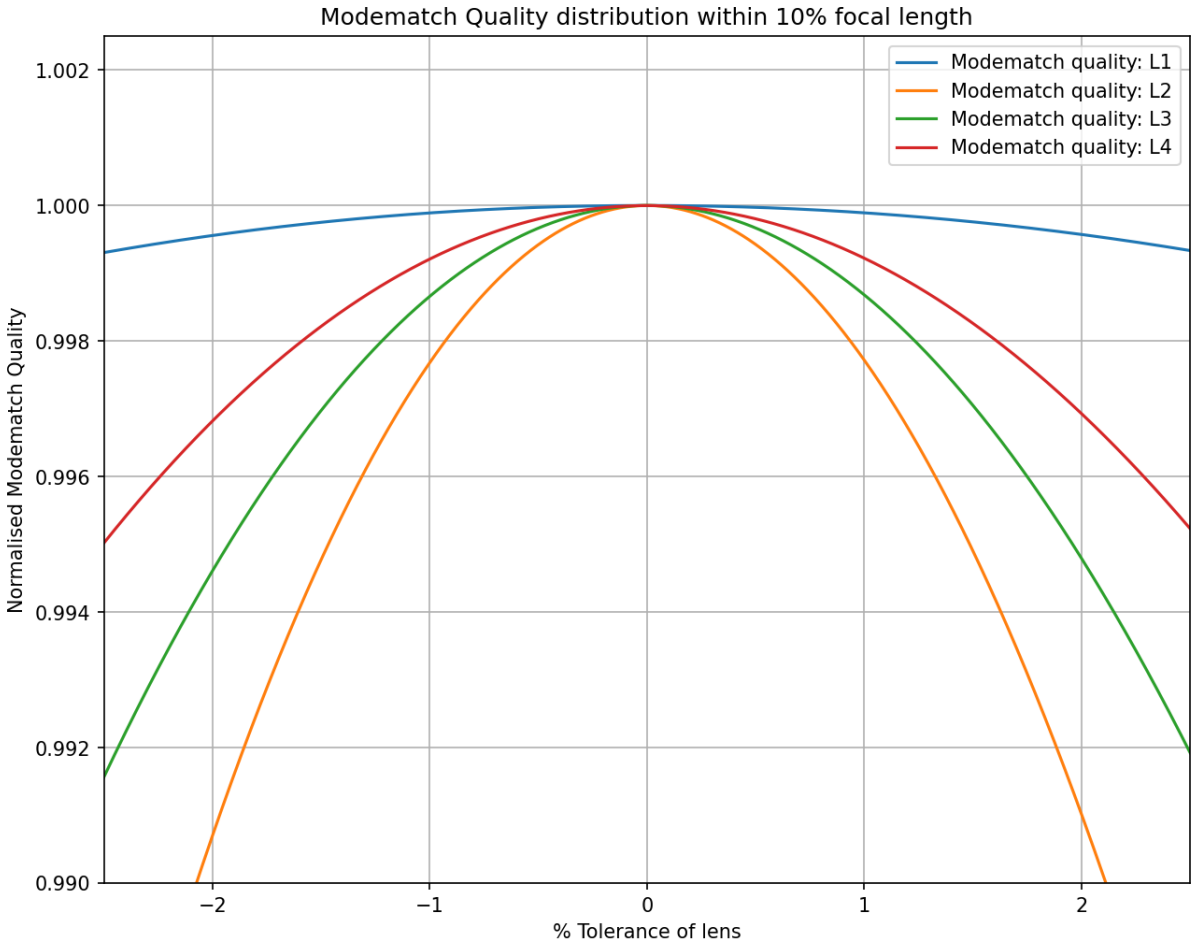

Figure 10b: An alternate view of the mode-matching values obtained for the cryogenic cavity. Plot details a high mode-matching percentage within a tolerance of 1%. Figure produced from [13].

Lenses 2 and 3 are critical to this setup. If either lenses 2 or 3 falls outside a tolerance of 5%, a mode-match of less than 99% is achieved. The solution presented for lenses 2 and 3 considers the manufacturing requirements as they are readily available from laserOptik. Lenses 1 and 4 can vary slightly in their construction; hence a condition of -0.430m and 0.350m is imposed, the latter readily available.

5.1.1. *Specification implications.* Overall, if the lens properties outlined for the cryogenic cavity are adhered to, a final difference in waist size of $0.1\mu m$ is observed with the proposed lenses. Similarly, for the reference cavity, a final difference in waist size of $7.43\mu m$ is observed with the setup described. Qualitatively this is a variance of 0.12% for the cryogenic cavity and 0.40% for the reference cavity.

5.2. Limitations on Approach

The main approximation to consider throughout this proposal is that of astigmatism. Additionally, lens locations and their adjustment can also hinder the setup's effectiveness. Lens locations were extremely restrictive within the tanks.

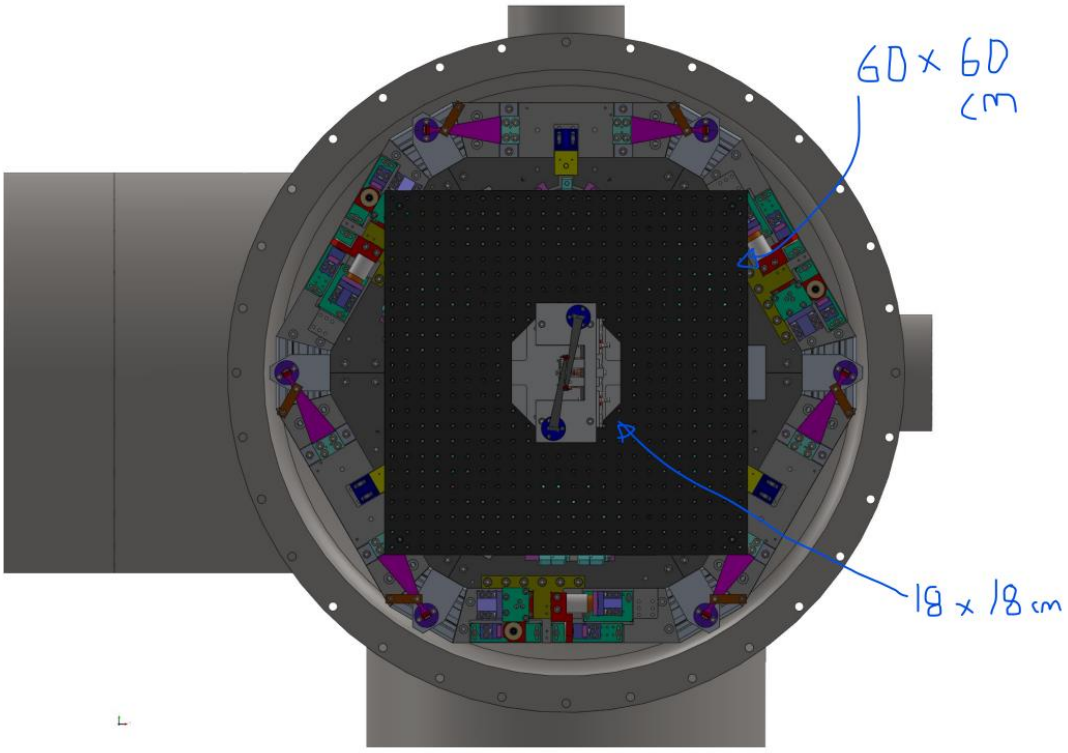

Figure 11: Zoomed in the cut-away rendering of a chamber of the apparatus. The enclosure consists of a mounting platform for lenses. [14]

As illustrated, each lens had a possible adjustment of +/- 30cm from origin. This limit was only further tightened within the final tank, the smaller of the three. Restricting lens locations restricted the number of possible solutions available. With the constraints applied to the lens locations, a further location had to be added within the cryostat chamber; otherwise, solutions would be impracticable.

5.2.1. *Astigmatism.* One major factor to consider was the effect of astigmatism. Essentially, it is an effect of Gaussian beam interaction with curved mirrors. The setup initially described is rectilinear, so this issue should be resolved assuming precise mirror alignment. Disregarding this effect can lead to improper mode-matching of the results hence delivering a more approximate final value for lens properties. The simulation does account for astigmatism, but it should not be deemed a priority assuming proper alignment.

5.3. Evaluation and improvements

With regards to code structure, multiple improvements could be made. This would decrease code runtime while also simplifying the design. A method could have been created for the cryogenic solution that optimizes for two lenses based on initial conditions. This method could then be called twice in a separate script, thus decreasing runtime and improving the structure.

The entire script for the reference cavity solution could be wrapped inside one function with inputs requiring initial waist size, final waist size and wavelength of light. This method would allow the user to specify what wavelength of light to use and potentially iterate over multiple wavelengths discovering new setups. Changing the script this way would serve more as a tool for researching various layouts exceedingly quickly.

A final improvement could be made to the alignment mechanisms for the lenses. A linear track may be used to acquire the precision necessary for some lens placement, specifically that of lens 1 for the cryogenic cavity. Using a linear track, a much more acceptable tolerance to lens positioning may be achieved rather than adjusting lens positions by hand.

A high level of confidence can be assumed for both lens location and lens properties due to the success of the mode-matching results. With a final difference of 0.1μm and 7.43μm for the waist sizes of the cryogenic and reference cavity, respectively, it can be stated that the solution provided was a success.

6. Conclusion

To summarise, this project aimed to achieve an optimal optical layout for a 10m cryogenic interferometer. This has been achieved by assessing the layout provided and constructing a python simulation of both cavities. This simulation solved for an exact solution for lens properties for each cavity. This exact solution was then iterated to find acceptable lens properties within manufacturing capabilities and provided the necessary waist sizes upon exit. Both manufactured and exact solutions were then compared via mode-matching and a result of upwards of 99% mode-matching was achieved. The final requirements for the reference cavity totals in at approximately £100 with focal lengths of -1.750m and 2.500m, respectively. Likewise, the final setup for the cryogenic cavity costs £160 with focal lengths of -0.430m, 1.875m, 2.500m and 0.350m for lenses 1 to 4, respectively. Improvements could optimize both the structure and runtime of the code used to simulate the cavities. With a difference of 0.1μm and 7.43μm attained for the cryogenic cavity and reference cavity, respectively it can be concluded that the proposed setup would be sufficient for experimentation.

References

[1] Abbott, B.P. et al., 2016. "Observation of Gravitational Waves from a Binary Black Hole Merger," *Physical Review Letters*, vol. 116, no. 6. DOI: https://doi.org/10.1103/PhysRevLett.116.061102

[2] "What are gravitational waves?", https://www.ligo.caltech.edu/page/what-are-gw Accessed: 30-10-2021

[3] Adhikari, R. X. et al., 2020. "A cryogenic silicon interferometer for gravitational-wave detection," *Classical and Quantum Gravity*, vol. 37, no. 16. DOI: https://doi.org/10.1088/1361-6382/ab9143

[4] Oelker, E., 2021 *Pictorial sketch of the 10m cryogenic interferometer*. [Pictorial Rendering]. At: Glasgow: Glasgow University.

[5] Degallaix, J. et al., 2013 "Bulk optical absorption of high resistivity silicon at 1550nm," *Optics Letters*, vol. 38, no. 12, pp. 2047-2049. DOI: https://doi.org/10.1364/OL.38.002047

[6] Brooker, G., 2003. Modern Classical Optics. 1st ed. New York: Oxford University Press Inc. pp. 173, 156-157. ISBN: 978-0198599654

[7] Alda, J., 2003. "Laser and Gaussian beam propagation and transformation," *Encyclopedia of optical engineering*, pp.1000. https://www.researchgate.net/publication/255041663_Laser_and_Gaussian_Beam_Propagation_and_Transformation Accessed: 10-10-2021

[8] Paschotta, R. "Gouy Phase Shift," https://www.rp-photonics.com/gouy_phase_shift.html Accessed: 03-11-2021

[9] Paschotta, R. "Mode Matching," https://www.rp-photonics.com/mode_matching.html Accessed: 03-11-2021

[10] Briggs, J. H., 2021 *"The Analysis, Experimental Characterization and Prototyping of Technologies for Making Quantum Noise Limited Detections of Gravitational Waves*," PhD thesis, University of Glasgow, Glasgow. pp 291-296

[11] "LaserOptik GmbH", https://www.laseroptik.com/ Accessed: 22-02-2022

[12] Dick, C. Webster, S. Oelker, E., *"Reference Cavity Solution"*, (2022), GitHub repository, https://github.com/swebster49/mode-matching-calculator/blob/b6562572d24bc2035d04d88d89ef486bbfbafadd/Reference%20Cavity%20Solution.py Updated: 25-03-2022

[13] Dick, C. Webster, S. Oelker, E., *"Cryogenic Cavity Solution"*, (2022), GitHub repository, https://github.com/swebster49/mode-matching-calculator/blob/2135a929f75e166a712b73deeeecf9d676a9ffdc/Cryogenic%20Cavity%20Solution.py Updated: 25-03-2022

[14] Oelker, E., 2021 *Zoomed in view of the chamber*. [C.A.D. Rendering]. At: Glasgow: Glasgow University.